Determination of Carbon Nanotube Density by Gradient Sedimentation

Qi Lu,[†] Gayatri Keskar,[‡] Razvan Ciocan,[†] Rahul Rao,[†] Rakesh B. Mathur,[§] Apparao M. Rao,[†] and Lyndon L. Larcom*[,†]

Department of Physics and Astronomy, Department of Materials Science and Engineering, Clemson University, Clemson, South Carolina 29634, and Carbon Technology Unit, National Physical Laboratory, New-Delhi-110012, India

Received: June 12, 2006; In Final Form: September 1, 2006

Density gradient centrifugation is a high-resolution technique for the separation and characterization of large molecules and stable complexes. We have analyzed various nanotube structures by preparative centrifugation in sodium metatungstate−water solutions. Bundled, isolated and acid-treated single-walled nanotubes (SWNTs) and multiwall nanotubes (MWNTs) formed sharp bands at well-defined densities. The structure of the material in each band was confirmed by transmission electron microscopy and Raman spectroscopy. Our data suggest respective densities of 1.87, 2.13, 1.74, and 2.1 g/cm^3 for bundled, isolated, and acid-treated SWNTs and MWNTs. These measured results compare well with their calculated densities.

1. Introduction

Carbon nanotubes (CNTs) are well-known for their physical properties and have found numerous applications due to their unique electrical, optical, thermal, and mechanical properties.[1] The solublization and functionalization of CNTs[2−4] have extended their applications into biological systems. However, a fundamental physical property, viz. the density of CNTs, has received little attention. Since density is closely related to the intrinsic structure of the CNT, it can be used to quantify the purification and separation of CNTs from the as-prepared soot. Moreover, since the presence of defects alters the structure of a CNT, the density may also serve as a measure of the quality of the CNTs. Certain CNT-based applications such as polymer composites with tailored properties and sensors that use the CNT as a nanosized cantilever could benefit from a detailed analysis of how the CNT density varies in its isolated or bundled forms. This study aims to provide a foundation for such analysis.

A single-walled carbon nanotube (SWNT) is formed when a single graphene sheet is wrapped into a seamless tube with a diameter of ∼1 nm. X-ray diffraction and electron microscopic studies have shown that bundled SWNTs are formed in the soot prepared by the pulsed laser vaporization and electric arc methods. The chirality specifies the details of how the graphene sheet is wrapped into a SWNT and leads to three classes of SWNTs: armchair, zigzag, and chiral nanotubes.[1] The unit cell of an individual SWNT is dependent on the chirality which leads to different lattice parameters and densities. For example, simulations by Gao et al.[5] found that the (10,10) armchair tubes possess a lattice parameter of $a_{(10,10)} = 16.78$ Å and a density of $\rho_{(10,10)} = 1.33$ g/cm^3. The corresponding values for a (17,0) zigzag tube are $a_{(17,0)} = 16.52$ Å and $\rho_{(17,0)} = 1.34$ g/cm^3, while $a_{(12,6)} = 16.52$ Å and $\rho_{(12,6)} = 1.40$ g/cm^3 for a chiral (12,6) tube. A multiwalled carbon nanotube (MWNT) is formed when SWNTs with increasing tube diameters self-assemble concentrically into a single carbon nanotube.[1] For a MWNT with an outer diameter of 8−15 nm and an inside diameter of 3−5 nm, the density is typically observed to be around 2.1 g/cm^3.[6]

Herein, we describe a process for determining the densities of CNTs using the equilibrium density gradient sedimentation method[7] which is widely used for measuring the densities or molecular weights of macromolecules, as well as for separating colloids and minerals. A sodium metatungstate−water solution is centrifuged to form a density gradient in the centrifugal field. The macromolecule sediments in the gradient to a position where the density of the macromolecule closely approximates the density of the solution. This technique can separate macromolecules with remarkably small differences in density. For example, in a standard centrifuge cell at 40 000 rpm using cesium chloride gradient solution, a density difference of 0.014 g/cm^3 in macromolecules results in a separation of about 0.5 mm.[7] In our study, sodium metatungstate ($Na_6[H_2W_{12}O_{40}]$, abbreviated as NamW) solutions were used to determine the densities of CNTs because of NamW's high density (3.12 g/cm^3 at 25 °C), low viscosity at high concentration, and high solubility in water.[7] For samples available in small amounts or low concentrations, this technique is more convenient and accurate than other conventional techniques.[8]

2. Methods and Materials

Gradient Centrifugation. NamW−water solution was obtained by adding NamW (2.82 g/mL, Acros Organics) to distilled water at a volume ratio of 7:9 (NamW/H_2O). Around 0.5 mg of CNTs was added to 3 mL of NamW−water solution in a Beckman polyallomer centrifuge tube (11mm × 60 mm). Centrifugation was performed with a Beckman SW56 rotor at 23 000 rpm and 20 °C. After 60 h of centrifugation, well-defined bands were formed whose distances from the meniscus were measured. The gradients were fractionated in 200-μL fractions, and each was weighed on a Mettler H20T balance.

Transmission Electron Microscopy (TEM). Fractionated CNT samples were stained with uranyl acetate and deposited on 300-mesh copper grids for TEM characterization with a Hitachi 7600 microscope.

Raman Spectroscopy. The micro-Raman data for SWNTs were gathered using a TRIAX 550 single-grating spectrometer

* To whom correspondence should be addressed. E-mail: lllrcm@clemson.edu.
[†] Department of Physics and Astronomy, Clemson University.
[‡] Department of Materials Science and Engineering, Clemson University.
[§] Carbon Technology Unit, National Physical Laboratory.

10.1021/jp063660k CCC: $33.50 © 2006 American Chemical Society
Published on Web 11/10/2006

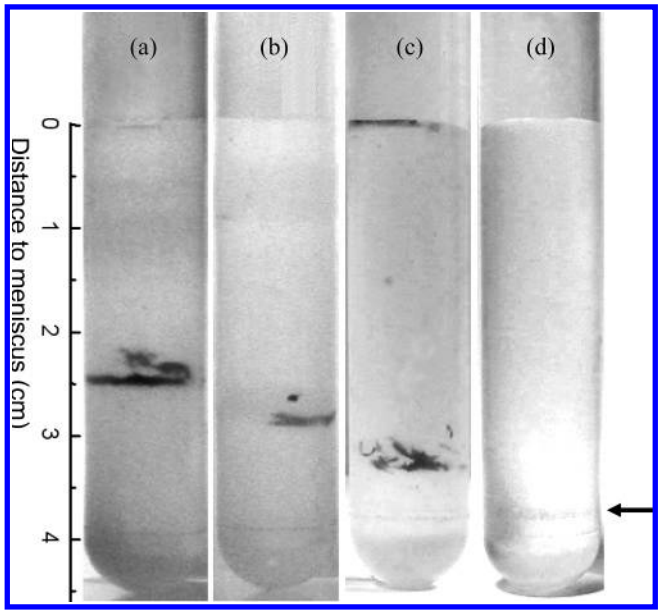

Figure 1. Different types of CNTs, (a) acid-SWNTs, (b) p-SWNT bundles, (c) MWNTs, and (d) iso-SWNTs, formed bands at different heights in gradients prepared under identical conditions. In (c), the band formed at the meniscus corresponds to amorphous carbon present in the MWNT sample. A barely visible band was observed in (d), and most iso-SWNTs seemed to aggregate at the height indicated by the left-pointing arrow.

(groove density 1 200 grooves/mm) equipped with a liquid nitrogen-cooled charge-coupled device (CCD). A Spectra-Physics Ar ion laser with a wavelength of 514.5 nm was used to excite Raman scattering from the CNTs.

CNT Samples. The pristine SWNT (p-SWNT) bundles and isolated SWNTs (iso-SWNT) used in this study were prepared by the electric arc discharge and chemical vapor deposition (CVD) methods, respectively.[1] Acid-treated SWNTs (acid-SWNT) were prepared by ultrasonic agitation of pristine SWNTs in a 3:1 mixture of concentrated H_2SO_4 and HNO_3. As a result of the treatment, SWNTs became soluble in water with abundant carboxyl end-groups generated at defect sites and terminals.[9] MWNTs were prepared using two methods: (i) from a thermal decomposition of a ferrocene−xylene mixture[10] and (ii) by striking an electrical arc discharge between two graphite electrodes in an inert atmosphere.[11]

3. Results and Discussion

Bands corresponding to various structures of CNTs are shown in Figure 1. The different structures sedimented to different levels in gradients prepared under identical conditions. The bands were confirmed to contain MWNTs, p-SWNT bundles, or iso-SWNTs using the Raman spectroscopic fingerprints demonstrated in Figure 2. In the Raman spectrum of iso-SWNTs, sharp radial breathing modes (RBM) are observed at 157 and 266 cm^{-1} which correspond to SWNT diameters of 1.58 and 0.93 nm, respectively.[12] The peaks present at ∼520 and ∼950 cm^{-1} correspond to the Raman modes of the Si substrate, and the G-band is observed at 1 588 cm^{-1} as expected.[1] In the Raman spectrum of arc-prepared MWNTs, a pronounced disorder-induced band (D-band) is also observed at 1357 cm^{-1} in addition to the G-band at 1 581 cm^{-1}. The p-SWNT bundles show the RBM and G-bands at 170 and 1 588 cm^{-1}, respectively.

Figure 3 shows the density profile along the length of a NamW gradient. The density data, obtained by weighing each

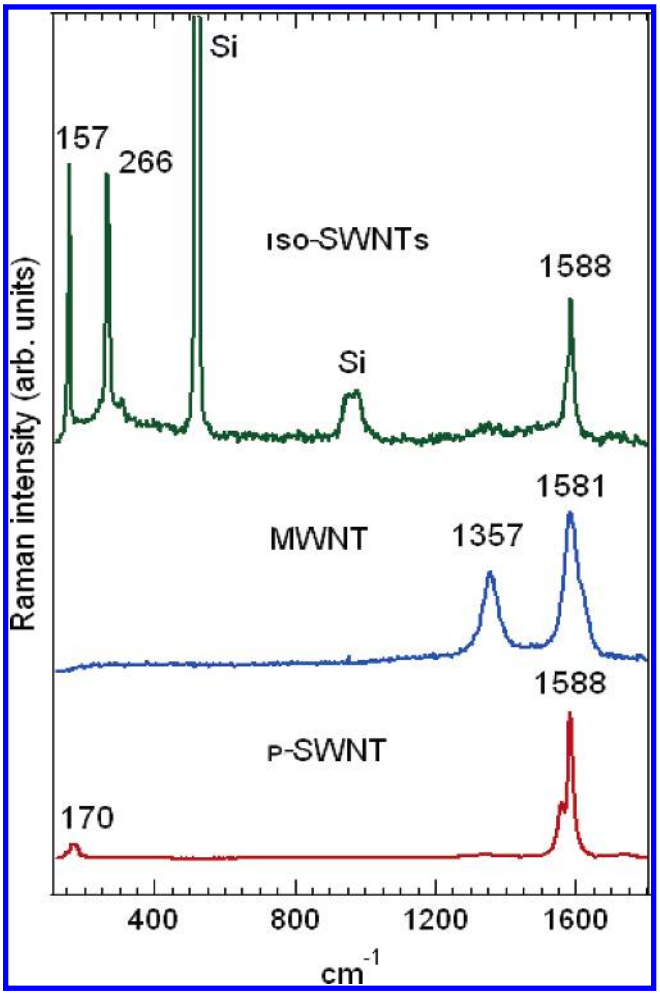

Figure 2. Raman characterization of p-SWNT bundles, MWNTs, and iso-SWNTs (see text).

gradient fraction of 200 μL, were fit to a straight line. The solid circle on the straight line indicates the position of the sharp band formed by the p-SWNT bundles (see Figure 1b). The corresponding density at this position in the gradient is 1.90 g/cm^3. The densities of other forms of SWNTs and MWNTs were measured using a similar approach and are presented in Table 1. The experimental deviation for the densities listed in Table 1 was obtained from three independent experiments. The deviation was calculated as

$$\sqrt{\sum(\rho - \bar{\rho})^2/(n-1)}$$

where ρ is the density measured for each experiment, $\bar{\rho}$ is the mean density, and n equals 3.

Extensive TEM studies were conducted to determine (i) diameter distribution of individual SWNTs within a p-SWNT bundle, (ii) distribution of p-SWNT bundle diameters, and (iii) distribution of MWNT diameters (Figure 4). From Gaussian analysis of the histograms shown in Figure 4, the mean diameters of individual tubes in p-SWNT bundles, of p-SWNT bundles, and of MWNTs were determined to be 1.44 ± 0.04, 8.00 ± 0.11, and 49.26 ± 2.16 nm, respectively. These experimentally determined diameters were used in the model described below to estimate the densities of p-SWNT bundles and MWNTs.

The density of an individual SWNT was computed by considering it as a rolled honeycomb sheet of length ***L*** and

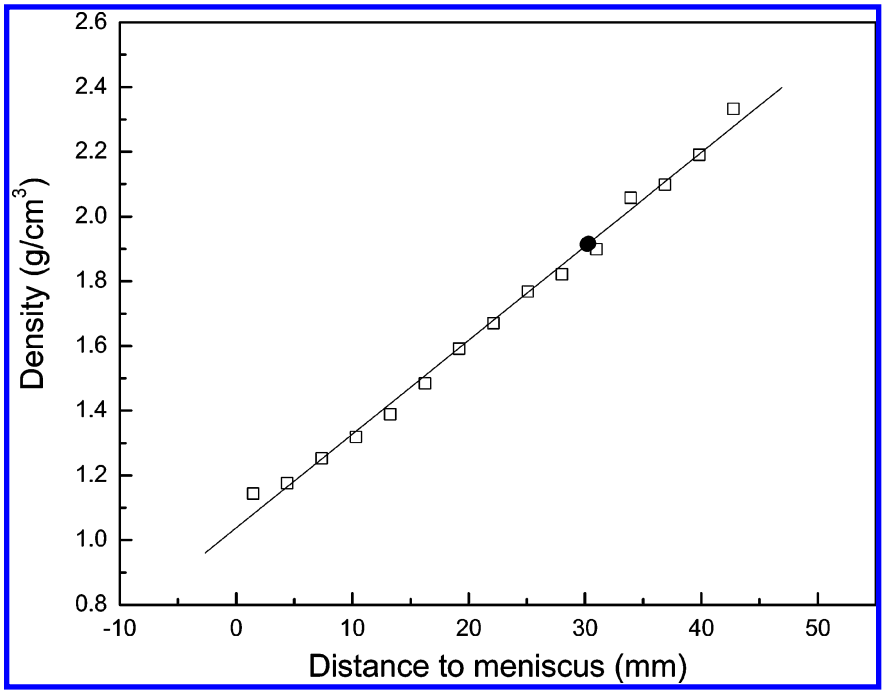

Figure 3. Density profile along the length of a NamW gradient. The density data, obtained by weighing each gradient fraction of 200 μL, fit a straight line of $y = 0.2903x + 1.0371$, where x is the distance from the meniscus to a particular fraction and y is its density. The solid circle on the trendline of the density gradient indicates the position of a sharp band corresponding to p-SWNTs. The density at this point in the gradient is 1.90 g/cm^3.

TABLE 1: Measured Densities of Various Forms of CNTs[a]

	acid-SWNT	p-SWNT	iso-SWNT	MWNT (CVD)	MWNT (Arc Discharge)
density (g/cm^3)	1.74 ± 0.04	1.87 ± 0.03	2.13 ± 0.04	2.09 ± 0.02	2.11 ± 0.03

[a] The data represent the means of three independent experiments, and the numbers following "±" are experimental deviations calculated as described in the text.

diameter $\boldsymbol{D}_{\mathrm{SWNT}}$. Density ρ_{SWNT} is given as

$$\rho_{\mathrm{SWNT}} = \frac{m}{V} = \frac{N_{\mathrm{C}} m_{\mathrm{C}}}{L\pi\frac{D_{\mathrm{SWNT}}^2}{4}} = \frac{\pi\frac{D_{\mathrm{SWNT}}\,L}{D_2\;\;D_2}}{L\pi\frac{D_{\mathrm{SWNT}}^2}{4}} Zu = \frac{4Zu}{D_{\mathrm{SWNT}} D_2^2} \qquad (1)$$

where N_{C} and m_{C} correspond to the number and mass of the carbon atoms. In eq 1, $D_2 = 2.83$ Å is the longest distance between carbon atoms in a single hexagonal lattice,[1] Z is the atomic mass for a carbon atom and u is the atomic mass unit (1.6605×10^{-27} kg). Following a similar rationale the density of a SWNT bundle can be written as

$$\rho_{\mathrm{Bundle}} = \frac{m}{V} = \frac{n_{\mathrm{SWNT}} N_{\mathrm{C}} m_{\mathrm{C}}}{L\pi\frac{D_{\mathrm{Bundle}}^2}{4}} = \frac{n_{\mathrm{SWNT}}\pi\frac{D_{\mathrm{SWNT}}\,L}{D_2\;\;D_2}}{L\pi\frac{D_{\mathrm{Bundle}}^2}{4}} Zu = \frac{4 n_{\mathrm{SWNT}} D_{\mathrm{SWNT}} Zu}{D_{\mathrm{Bundle}}^2 D_2^2} \qquad (2)$$

where D_{Bundle} is the bundle diameter which can be expressed as

$$D_{\mathrm{Bundle}} = D_{\mathrm{SWNT}}(2n_{\mathrm{tier}} + 1) + 2n_{\mathrm{tier}} D_{\mathrm{il}} \qquad (3)$$

The variable $n_{\mathrm{SWNT}} = 1, 7, 19, 37, 61$ is the number of SWNTs in each tier, n_{tier} is the number of tiers for each bundle, and $D_{\mathrm{il}} = 3.38$ Å is the interlayer spacing shown in Figure 5a.[1]

As indicated in the caption to Figure 4, the samples used in this study were assumed to fit a Gaussian distribution in diameters for individual tubes and for p-SWNT bundles. Therefore, we express the $n_{\mathrm{SWNT}}D_{\mathrm{SWNT}}$ term in eq 2 for a SWNT bundle as

$$n_{\mathrm{SWNT}} D_{\mathrm{SWNT}} = \sum_{i=1}^{n} A_i D_i \exp\left(-\frac{(D_i - D_o)^2}{2\sigma^2}\right) \qquad (4)$$

where A_i, D_i, D_o, and σ are obtained from a Gaussian fit to the experimental diameter distribution of individual SWNTs within a bundle (see Figure 4).[13] A_i, D_i, D_o and σ correspond to the weighting factor, binning diameter, median diameter and the standard deviation, respectively. Substituting eq 4 in eq 2 gives

$$\rho_{\mathrm{Bundle}} = \frac{4Zu}{D_{\mathrm{Bundle}}^2 D_2^2} \sum_{i=1}^{n} A_i D_i \exp\left(-\frac{(D_i - D_o)^2}{2\sigma^2}\right) \qquad (5)$$

It is a well-known fact that residual catalysts are present in p-SWNT bundles. Next we discuss how the presence of catalyst particles can be taken into account in our model calculations. We consider the measured density of p-SWNT bundles (ρ_{measured}) in terms of the density and volume of SWNT bundles and

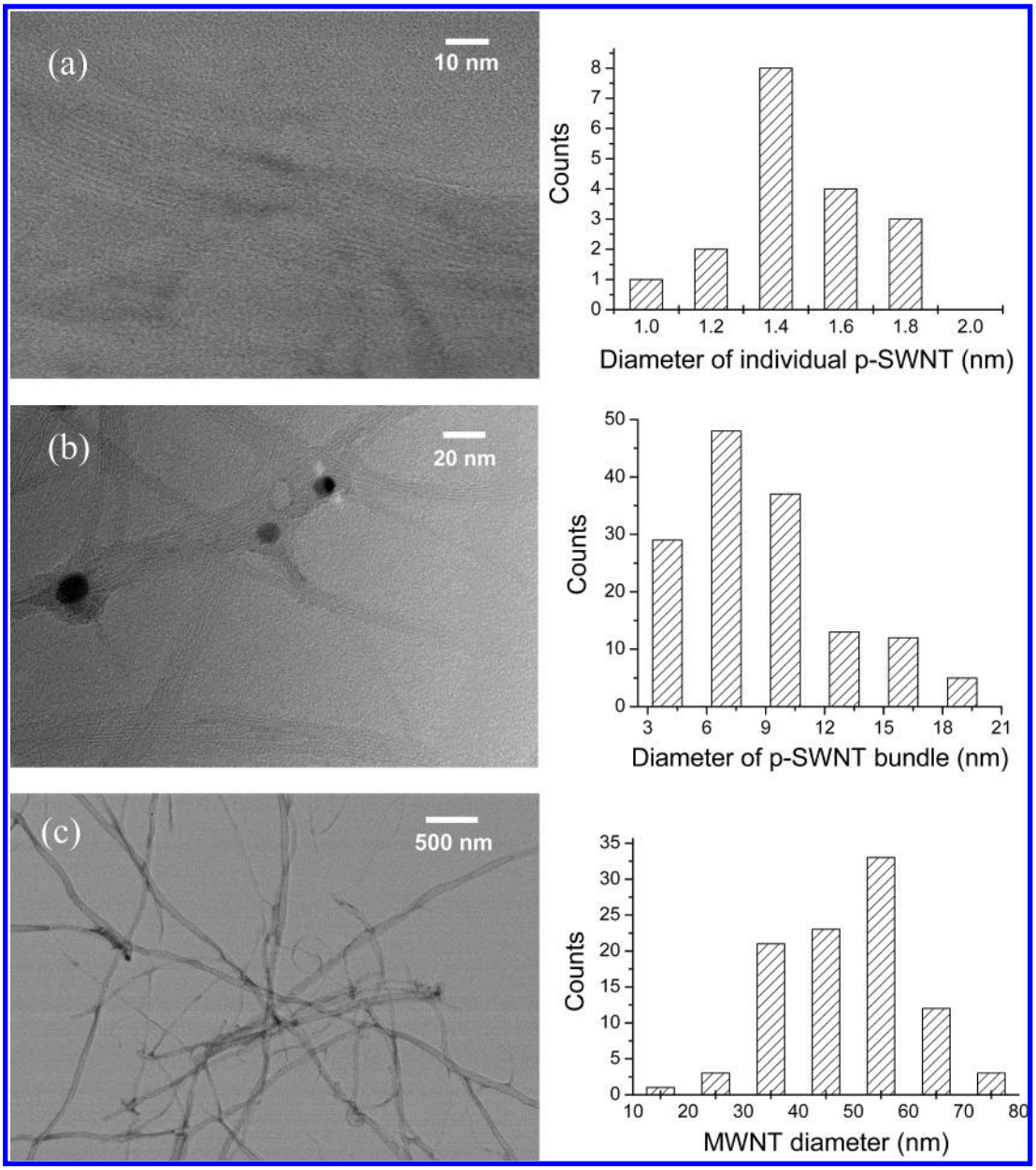

Figure 4. TEM images of (a) individual SWNTs inside a p-SWNT bundle, (b) p-SWNT bundles, and (c) MWNTs. Diameter distributions for each of these structures were determined from TEM images. From Gaussian analysis of the diameter distributions, the mean diameters of individual p-SWNTs, p-SWNT bundles, and MWNTs were determined to be 1.44 ± 0.04, 8.00 ± 0.11 and 49.26 ± 2.16 nm, respectively.

catalyst particles as follows:

$$\rho_{\text{measured}} = \frac{m}{V} = \frac{m_{\text{Carbon}} + m_{\text{Catalyst}}}{V_{\text{Bundle}}} = \frac{m_{\text{Carbon}} + m_{\text{Catalyst}}}{\frac{m_{\text{Carbon}}}{\rho_{\text{Bundle}}}} =$$

$$\rho_{\text{Bundle}} \frac{m_{\text{Carbon}} + m_{\text{Catalyst}}}{m_{\text{Carbon}}} = \rho_{\text{Bundle}} \left(1 + \frac{m_{\text{Catalyst}}}{m_{\text{Carbon}}}\right) \quad (6)$$

In eq 6, we neglect the volume of the catalyst in comparison to the volume of the SWNT bundles. The quantity $m_{\text{Catalyst}}/m_{\text{Carbon}}$ was taken to be 0.26 from the atomic composition of the anode (C = 95 atom %; Ni = 4 atom %; Y = 1 atom %). Using eq 5, the densities of SWNT bundles with bundle diameters ranging from 1 to 15 nm were calculated. These are plotted in Figure 5b (dashed line passing through open triangles). When residual catalyst particles present in the SWNT bundles were taken into account, the calculated densities (solid line passing through crosses in Figure 5b) were computed as described by eq 6. The experimentally determined densities of iso-SWNTs, acid-SWNTs, and p-SWNT bundles are also plotted in the same figure. They agree reasonably well with the computed densities represented by the solid trace. This observation is consistent with the presence of catalyst particles in the p-SWNT bundles as revealed in the TEM images (Figure 4). Furthermore, our calculated density for a SWNT bundle in the absence of catalyst particles is in good agreement with that reported from a molecular dynamic simulation for a bundle of SWNTs with an overall bundle diameter of 10 nm.[5]

Next we focus on the model calculation for the density of MWNTs. The density of a MWNT can be computed in the continuum limit in which a MWNT is treated as a cylinder of thickness h and length L.[14] Therefore, the MWNT density can

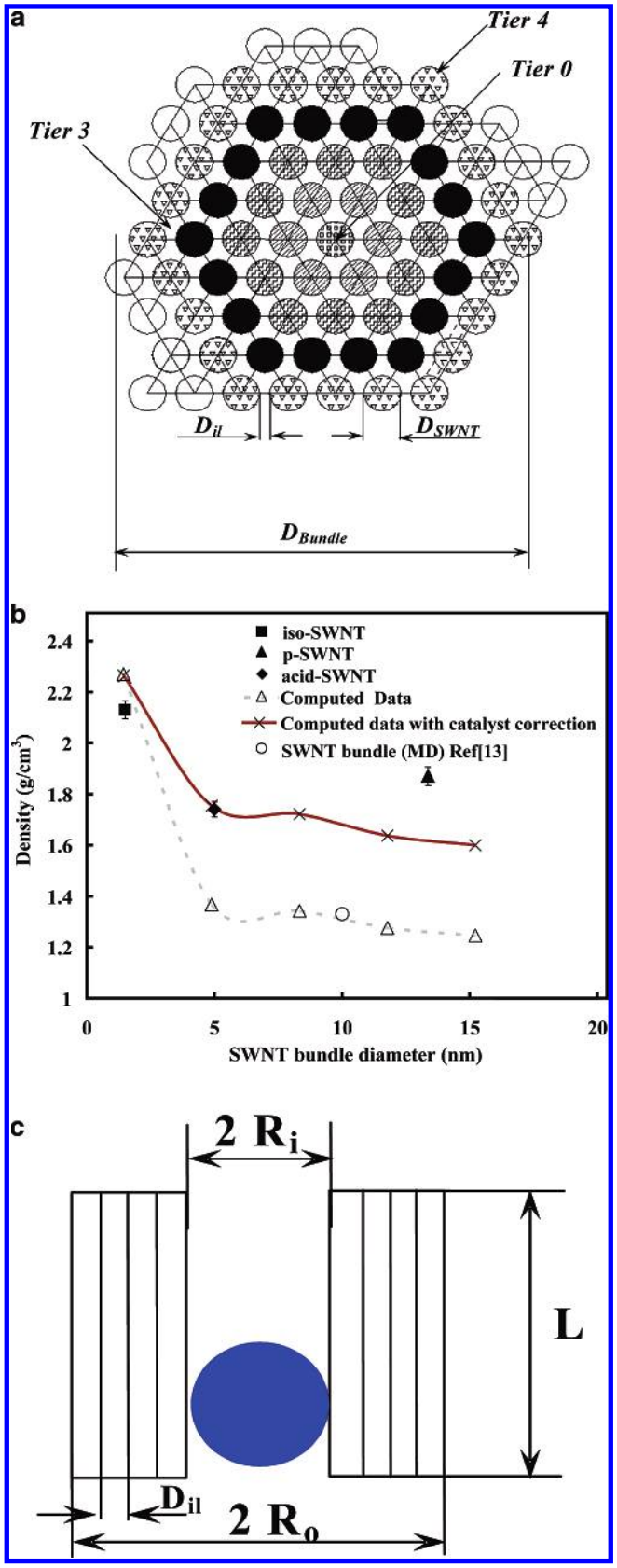

Figure 5. (a) Density of SWNT bundles was computed based on the arrangement of individual SWNTs in tiers. (b) Density of SWNTs plotted as a function of the diameter of bundles. Both computational (crosses, open triangles, and open circle) and experimental (solid square, solid triangle, and solid diamond) densities are presented. (c) Illustration of MWNT based on continuum hypothesis. The multishells are treated as continuum media each with thickness h and length L.

TABLE 2: Measured and Computed Densities of MWNTs Compared with Those Reported in the Literature

density (g/cm^3)	outer tube diameter (nm)	inner tube diameter (nm)	source
2.16	33.6	~10	ref 6
~2.1	8−15	3−5	ref 15
2.14	50	10	model (this work)
2.09	48	~10	measured density for CVD-grown MWNTs (this work)
2.11	50	~15	measured density for electric arc-grown MWNTs (this work)

be expressed as

$$\rho_{\mathrm{MWNT}} = \frac{m}{V} = \frac{m_{\mathrm{MWNT}}}{V_{\mathrm{MWNT}}} = \frac{\rho_{\mathrm{graphite}} \sum V_{\mathrm{w}_i}}{L\pi(R_{\mathrm{o}}^2 - R_{\mathrm{i}}^2)} = \frac{\rho_{\mathrm{graphite}} hL \sum_{i=1}^{n_{\mathrm{w}}} \pi D_{\mathrm{w}_i}}{L\pi(R_{\mathrm{o}}^2 - R_{\mathrm{i}}^2)} \quad (7)$$

where ρ_{graphite} and h are the density and thickness of a single graphite layer (graphene). D_{wi} corresponds to the diameter of the ith wall in the MWNT. R_{i} and R_{o} define the inner and outer radii of the MWNT (Figure 5c). High-resolution TEM studies showed that the interlayer space for a MWNT ranges from 0.34 to 0.39 nm, which increases with decreasing tube diameter.[13] The distance D_{il} from one shell to the neighboring shell of a MWNT with diameter D is given by[13]

$$D_{\mathrm{il}} = 0.344 + 0.1\, \mathrm{e}^{-D/2} \quad (8)$$

Note the diameters in eq 8 are in nanometers. The diameter of a MWNT with "i" number of walls is given by

$$D_{\mathrm{w}_i} = 2R_{\mathrm{i}} + 2(i-1)D_{\mathrm{il}} = 2R_{\mathrm{i}} + 2(i-1)\left(0.344 + 0.1 \exp\left(-\frac{D_{\mathrm{w}_{i-1}}}{2}\right)\right)10^9 \quad (9)$$

where we have substituted eq 8 in eq 9 so that the diameter of a MWNT with i number of walls is expressed in terms of the diameter of the $(i-1)$th wall. With eqns 8 and 9 substituted in eq 7, it follows that

$$\rho_{\mathrm{MWNT}} = \frac{h\rho_{\mathrm{graphite}} \sum_{i=1}^{n_{\mathrm{w}}} \left[2R_{\mathrm{i}} + 2(i-1)\left(0.344 + 0.1 \exp\left(-\frac{D_{\mathrm{w}_{i-1}}}{2}\right)\right)10^9\right]}{(R_{\mathrm{o}}^2 - R_{\mathrm{i}}^2)} \quad (10)$$

As in the case of SWNTs, the presence of the catalyst particles needs to be considered before we compare our calculated densities to those obtained in our experiments. In MWNTs, the presence of the catalyst particles can be taken into account by

$$\rho_{\mathrm{measured}} = \rho_{\mathrm{MWNT}}\left(1 + \frac{m_{\mathrm{Catalyst}}}{m_{\mathrm{Carbon}}}\right) \quad (11)$$

The density of a MWNT preparation whose diameter distribution is shown in Figure 4c is calculated as 2.14 g/cm^3 using eq 11. This value is in good agreement with the densities reported in refs 6 and 15 as shown in Table 2. In this study, the densities

of MWNTs synthesized by CVD and electrical arc discharge were measured to be 2.09 and 2.11 g/cm^3, respectively.

The density of acid-SWNTs was measured to be 1.74 ± 0.04 g/cm^3, which is 0.13 g/cm^3 less than the density of p-SWNT bundles (see parts a and b of Figure 1). A structural transformation from p-SWNT to acid-SWNTs bundles would produce such a decrease in density. A close-packed triangular lattice formed by individual tubes in p-SWNT bundles was disrupted by acidic oxidation under the shock of localized ultrasonic bubbling. The carboxyl groups generated at the ends and sides of the tubes caused individual tubes to become hydrophilic and separated from one another in the water network. The scattered spatial disposition reduces the density. In the case of MWNTs, we observed two bands (Figure 1c): one close to the meniscus corresponding to amorphous carbon (consistent with the presence of a strong D-band in the Raman spectrum) and the other corresponding to MWNTs. However, among all CNT structures, iso-SWNTs have the highest density (Figure 1d).

4. Conclusions

The densities of CNTs having various structures were measured with the equilibrium density gradient sedimentation technique using sodium metatungstate as the gradient-generating agent. The differences in structural features of CNTs result in distinguishable differences in densities. These were found to be in agreement with theoretical computations based on their structures.

Acknowledgment. This research work was supported by the NSF Grant No. DMI-0210559.

References and Notes

(1) Terrones, M. *Annu. Rev. Mater. Res.* **2003**, *33*, 419−501.

(2) Chen, J.; Hui, H.; Chen, Y.; Rao, A. M.; Eklund, P. C.; Haddon, R. C. *Science* **1998**, *282*, 95−98.

(3) Tasis, D.; Tagmatarchis, N.; Bianco, A.; Prato, M. *Chem. Rev.* **2006**, *106*, 1105−1136.

(4) Ciraci, S.; Dag, S.; Yildirim, T.; Gulseren, O.; Senger, R. T. *J. Phys.*: *Condens. Matter* **2004**, *16*, R901−R960.

(5) Gao, G.; Cagin, T.; Goddard, W. A. *Nanotechnology* **1998**, *9*, 184−191.

(6) Huang, Q.; Gao, L.; Liu, Y.; Sun, J. *J. Mater. Chem.* **2005**, *15*, 1995−2001.

(7) Plewinsky, B.; Kamps, R. *Makromol. Chem.* **1984**, *185*, 1429−1439.

(8) *Manual of Weighing Applications, Part 1;* Sartorius AG: Gottingen, Germany, 2004. See http://www.sartorius.com/fileadmin/sartorius_pdf/Prospekt/englisch/DensityDeterminationManual.pdf.

(9) Williams, K. A.; Veenhuizen, P. T. M.; Torre, B. G. de la; Eritja, R.; Dekker, C. *Nature (London)* **2002**, *420*, 761.

(10) Andrews, R.; Jacques, D.; Rao, A. M.; Derbyshire, F.; Qian, D.; Fan, X.; Dickey E. C.; Chen, J. *Chem. Phys. Lett.* **1999**, *303*, 467−474.

(11) Mathur, R. B.; Lal, C.; Dhami, T. L.; Seth, R. K. *National Conf. on Carbon, Indo-Carbon* **2001**, 226.

(12) Rao, A. M.; Richter, E.; Bandow, S.; Chase, B.; Eklund, P. C.; Williams, K. A.; Fang, S.; Subbaswamy, K. R.; Menon, M.; Thess, A.; Smalley, R. E.; Dresselhaus, G.; Dresselhaus, M. S. *Science* **1997**, *275*, 187−191.

(13) Kiang, C. H.; Endo, M.; Ajayan, P.; Dresselhaus, G.; Dresselhaus, M. *Phys. Rev. Lett.* **1998**, *81*, 1869−1872; http://www.wag.caltech.edu/foresight/foresight_2.html.

(14) Govindjee S.; Sackman, J. L. *Solid State Commun.* **1999**, *110*, 227−230.

(15) Qian, D.; Dickey, E. C.; Andrews, R.; Rantell, T. *Appl. Phys. Lett.* **2000**, *76*, 2868−2870.